

## Theoretical Investigations on the Formation and Dehydrogenation Reaction Pathways of $\text{H}(\text{NH}_2\text{BH}_2)_n\text{H}$ ( $n = 1-4$ ) Oligomers: Importance of Dihydrogen Interactions

Jun Li,<sup>\*,†,‡</sup> Shawn M. Kathmann,<sup>‡</sup> Han-Shi Hu,<sup>†</sup> Gregory K. Schenter,<sup>‡</sup> Tom Autrey,<sup>‡</sup> and Maciej Gutowski<sup>‡,§</sup>

<sup>†</sup>Department of Chemistry, Tsinghua University, Beijing 100084, China, <sup>‡</sup>W. R. Wiley Environmental Molecular Sciences Laboratory and Chemical and Materials Sciences Division, Pacific Northwest National Laboratory, Richland, Washington 99352, and <sup>§</sup>Chemistry-School of Engineering and Physical Sciences, Heriot-Watt University, Edinburgh EH14 4AS, U.K.

Received March 2, 2010

The  $\text{H}(\text{NH}_2\text{BH}_2)_n\text{H}$  oligomers are possible products from dehydrogenation of ammonia borane ( $\text{NH}_3\text{BH}_3$ ) and ammonium borohydride ( $\text{NH}_4\text{BH}_4$ ), which belong to a class of boron–nitrogen–hydrogen ( $\text{BNH}_x$ ) compounds that are promising materials for chemical hydrogen storage. Understanding the kinetics and reaction pathways of formation of these oligomers and their further dehydrogenation is essential for developing  $\text{BNH}_x$ -based hydrogen storage materials. We have performed computational modeling using density functional theory (DFT), *ab initio* wave function theory, and Car–Parrinello molecular dynamics (CPMD) simulations on the energetics and formation pathways for the  $\text{H}(\text{NH}_2\text{BH}_2)_n\text{H}$  ( $n = 1-4$ ) oligomers, polyaminoborane (PAB), from  $\text{NH}_3\text{BH}_3$  monomers and the subsequent dehydrogenation steps to form polyiminoborane (PIB). Through computational transition state searches and evaluation of the intrinsic reaction coordinates, we have investigated the B–N bond cleavage, the reactions of  $\text{NH}_3\text{BH}_3$  molecule with intermediates, dihydrogen release through intra- and intermolecular hydrogen transfer, dehydrocoupling/cyclization of the oligomers, and the dimerization of  $\text{NH}_3\text{BH}_3$  molecules. We find that the formation of  $\text{H}(\text{NH}_2\text{BH}_2)_{n+1}\text{H}$  oligomers occurs first through reactions of the  $\text{H}(\text{NH}_2\text{BH}_2)_n\text{H}$  oligomers with  $\text{BH}_3$  followed by reactions with  $\text{NH}_3$  and the release of  $\text{H}_2$ , where the  $\text{BH}_3$  and  $\text{NH}_3$  intermediates are formed through dissociation of  $\text{NH}_3\text{BH}_3$ . We also find that the dimerization of the  $\text{NH}_3\text{BH}_3$  molecules to form cyclic  $c\text{-(NH}_2\text{BH}_2)_2$  is slightly exothermic, with an unexpected transition state that leads to the simultaneous release of two  $\text{H}_2$  molecules. The dehydrogenations of the oligomers are also exothermic, typically by less than 10 kcal/(mol of  $\text{H}_2$ ), with the largest exothermicity for  $n = 3$ . The transition state search shows that the one-step direct dehydrocoupling cyclization of the oligomers is not a favored pathway because of high activation barriers. The dihydrogen bonding, in which protic ( $\text{H}_\text{N}$ ) hydrogens interact with hydridic ( $\text{H}_\text{B}$ ) hydrogens, plays a vital role in stabilizing different structures of the reactants, transition states, and products. The dihydrogen interaction (DHI) within the  $\text{R-BH}_2(\eta^2\text{-H}_2)$  moiety accounts for both the formation mechanisms of the oligomers and for the dehydrogenation of ammonia borane.

### Introduction

Hydrogen storage presents challenging bottlenecks in the development of a hydrogen economy.<sup>1–4</sup> Boron–nitrogen–hydrogen ( $\text{BNH}_x$ ) materials such as ammonia borane ( $\text{NH}_3\text{BH}_3$ )<sup>5,6</sup> are potentially important candidates for hydrogen

storage and catalytic hydrogen release because of their high hydrogen gravimetric and volumetric densities.<sup>7–12</sup> While the mechanisms of catalytic and thermal decomposition of ammonia borane have been investigated in both the gas and the

\*To whom correspondence should be addressed. E-mail: junli.thu@gmail.com.

(1) Satyapal, S.; Petrovic, J.; Read, C.; Thomas, G.; Ordaz, G. *Catal. Today* **2007**, *120*, 246.  
(2) Schlapbach, L.; Züttel, A. *Nature* **2001**, *414*, 353.  
(3) Grochala, W.; Edwards, P. P. *Chem. Rev.* **2004**, *104*, 1283.  
(4) Felderhoff, M.; Weidenthaler, C.; Helmolt, R.; Eberle, U. *Phys. Chem. Chem. Phys.* **2007**, *9*, 2643.  
(5) Shore, S. G.; Parry, R. W. *J. Am. Chem. Soc.* **1955**, *77*, 6084.  
(6) Heldebrant, D. J.; Karkamkar, A.; Linehan, J. C.; Autrey, T. *Energy Environ. Sci.* **2008**, *1*, 156.

(7) Wolf, G.; Baumann, J.; Baitalow, F.; Hoffmann, F. P. *Thermochim. Acta* **2000**, *343*, 19. Chandra, M.; Xu, Q. *J. Power Sources* **2006**, *156*, 190.  
(8) Baitalow, F.; Baumann, J.; Wolf, G.; Jaenicke-Rossler, K.; Leitner, G. *Thermochim. Acta* **2002**, *391*, 159.  
(9) Jacquemin, D.; Perpète, E. A.; Wathelet, V.; Andre, J.-M. *J. Phys. Chem. A* **2004**, *108*, 9616.  
(10) Gutowska, A.; Li, L.; Shin, Y.; Wang, C.; Li, S.; Linehan, J. R.; Smith, S.; Kay, B.; Schmid, B.; Shaw, W.; Gutowski, M.; Autrey, T. *Angew. Chem., Int. Ed.* **2005**, *44*, 3578.  
(11) Dixon, D. A.; Gutowski, M. *J. Phys. Chem. A* **2005**, *109*, 5129.  
(12) Hamilton, C. W.; Baker, R. T.; Staubitze, A.; Manners, I. *Chem. Soc. Rev.* **2009**, *38*, 279.

condensed phases,<sup>13–32</sup> the mechanism for the formation and decomposition of the corresponding  $\text{H}(\text{NH}_2\text{BH}_2)_n\text{H}$  oligomers has not been understood previously. The usefulness of  $\text{BNH}_x$  as hydrogen storage materials depends, among other things, on the kinetics and thermodynamics of dehydrogenation. Therefore, one of the key problems in investigating  $\text{BNH}_x$  as hydrogen storage materials is to understand the formation mechanisms, reactivities, reaction energetics, and dehydrogenation and reversed hydrogenation pathways in these materials. The  $\text{H}(\text{NH}_2\text{BH}_2)_n\text{H}$  oligomers (or polyaminoborane, PAB), products of dehydrocoupling of  $\text{NH}_3\text{BH}_3$ , are thus a good starting point for understanding the thermodynamics, dynamics, and kinetics of the  $\text{BNH}_x$  materials at a molecular level.

We previously investigated the geometries and thermodynamic stabilities of the chain, branched, and coiled structures of the  $\text{H}(\text{NH}_2\text{BH}_2)_n\text{H}$  ( $n = 1–6$ ) oligomers using Car–Parrinello molecular dynamics (CPMD) simulations and molecular density functional theory (DFT) calculations.<sup>33</sup> We found that the coiled structures, in which the  $\text{NH}_3$  and  $\text{BH}_3$  groups of the oligomers come together to form a head-to-tail geometry, and some branched structures are more stable than the linear chain structures and the triplet-state structures with a biradical character. While these theoretical investigations of oligomers provided information about their structures and thermodynamic stabilities, the mechanisms and kinetics of the formation and dehydrogenation of these oligomers still remain to be determined.

In this paper, we focus on the mechanisms of oligomer formation and decomposition of  $\text{H}(\text{NH}_2\text{BH}_2)_n\text{H}$  ( $n = 1–4$ ).

Using molecular DFT calculations and CPMD simulations, we have performed theoretical studies of the formation mechanisms of the oligomers and on several dehydrogenation pathways and their transition states, reaction energetics, and kinetic barriers for dehydrocoupling reactions of the oligomers. It is found that at low temperature the dehydrocoupling of the oligomers may occur via B–N bond cleavage and hydrogen-transfer intermediates, while direct dehydrocoupling cyclization of the oligomers is less likely to proceed through a one-step dehydrogenation because of the high activation barriers. We also show that it is ubiquitous in the transition states, intermediates, and the oligomers to form the  $\text{R–BH}_2(\eta^2\text{-H}_2)$  moiety by the  $\text{H}_\text{N} \rightarrow \text{H}_\text{B}$  hydrogen-transfer, which we call a *dihydrogen interaction* (DHI) on boron. This DHI can also be characterized as the interaction between nucleophilic and electrophilic hydrogen atoms.

## Computational Methods

The electronic structure calculations were performed at the DFT level using the Amsterdam Density Functional (ADF) code (version 2009.01).<sup>34</sup> The generalized gradient approach (GGA) with exchange–correlation functional of Perdew–Wang 1991 (PW91) was used,<sup>35</sup> as this functional performs well for ammonia borane systems from our previous work.<sup>33</sup> Uncontracted Slater basis sets of triple- $\zeta$  quality plus two polarization functions (TZ2P) were employed, which include d- and f-type polarization functions for B and N, and p- and d-type polarization functions for H.<sup>36</sup> To obtain accurate geometries, high numerical accuracy was used for the integration (Integration = 8.0) and a tight criterion was used for the energy convergence ( $10^{-8}$  a.u.) during the self-consistent field iterations. The geometries of the reactants, transition states, intermediates, and products were fully optimized until the energy gradients converged to within  $10^{-4}$  a.u. For very flat potential energy surfaces, we further tightened the energy gradients convergence to within  $10^{-5}$  a.u. to eliminate numerical noise in the energy and frequency calculations.

Transition states were located at the PW91 level of theory using the climbing image-nudged elastic band (CI-NEB) method implemented in ADF.<sup>34,37</sup> Some of the transition-states for dihydrogen release and B–N bond cleavage were initially determined via CI-NEB at the AM1 level of theory implemented in MOPAC<sup>38</sup> and the quasi-synchronous transit method (QST3) in Gaussian 98.<sup>39</sup> For consistency, these transition states geometries were subsequently refined using a mode-following algorithm from ADF.<sup>34</sup> Starting from the

(13) Hu, M. G.; Geanangel, R. A.; Wendlandt, W. W. *Thermochim. Acta* **1978**, *23*, 249.

(14) Wang, J. S.; Geanangel, R. A. *Inorg. Chim. Acta* **1988**, *148*, 185.

(15) Sit, V.; Geanangel, R. A.; Wendlandt, W. W. *Thermochim. Acta* **1987**, *113*, 379.

(16) Stowe, A. C.; Shaw, W. J.; Linehan, J. C.; Schmid, B.; Autrey, T. *Phys. Chem. Chem. Phys.* **2007**, *9*, 1831.

(17) Nguyen, V. S.; Matus, M. H.; Grant, D. J.; Nguyen, M. T.; Dixon, D. A. *J. Phys. Chem. A* **2007**, *111*, 8844.

(18) Nutt, W. R.; McKee, M. L. *Inorg. Chem.* **2007**, *46*, 7633.

(19) Palumbo, O.; Paolone, A.; Rispoli, P.; Cantelli, R.; Autrey, T. *J. Power Sources* **2010**, *195*, 1615.

(20) Zimmerman, P. M.; Paul, A.; Zhang, Z.; Musgrave, C. B. *Inorg. Chem.* **2009**, *48*, 1069.

(21) Kuznesof, P. M.; Shriver, D. F.; Stafford, F. E. *J. Am. Chem. Soc.* **1968**, *90*, 2557.

(22) Pusatcioglu, S. Y.; McGee, H. A., Jr.; Fricke, A. L.; Hassler, J. C. *J. Polym. Sci.* **1971**, *21*, 1561.

(23) Bluhm, M. E.; Bradley, M. G.; Butterick, R.; Kusari, U.; Sneddon, L. G. *J. Am. Chem. Soc.* **2006**, *128*, 7748.

(24) Nguyen, V. S.; Matus, M. H.; Nguyen, M. T.; Dixon, D. A. *J. Phys. Chem. C* **2007**, *111*, 9603.

(25) Shaw, W. J.; Linehan, J. C.; Szymczak, N. K.; Heldebrant, D. J.; Yonker, C.; Camaioni, D. M.; Baker, R. T.; Autrey, T. *Angew. Chem., Int. Ed.* **2008**, *47*, 7493.

(26) Heldebrant, D. J.; Karkamkar, A.; Hess, N. J.; Bowden, M.; Rassat, S.; Zheng, F.; Rappe, K.; Autrey, T. *Chem. Mater.* **2008**, *20*, 5332.

(27) Neiner, D.; Karkamkar, A.; Linehan, J. C.; Arey, B.; Autrey, T.; Kauzlarich, S. M. *J. Phys. Chem. C* **2009**, *113*, 1098.

(28) Bowden, M.; Autrey, T.; Brown, I.; Ryan, M. *Curr. Appl. Phys.* **2008**, *8*, 498.

(29) Sephiri, S.; Feaver, A.; Shaw, W. J.; Howard, C. J.; Zhang, Q. F.; Autrey, T.; Cao, G. Z. *J. Phys. Chem. B* **2007**, *111*, 14285.

(30) Fulton, J. L.; Linehan, J. C.; Autrey, T.; Balasubramanian, M.; Chen, Y.; Szymczak, N. K. *J. Am. Chem. Soc.* **2007**, *129*, 11936.

(31) Rousseau, R.; Schenter, G. K.; Fulton, J. F.; Linehan, J. C.; Autrey, T. *J. Am. Chem. Soc.* **2009**, *131*, 10516.

(32) Dietrich, B. L.; Goldberg, K. I.; Heinekey, D. M.; Autrey, T.; Linehan, J. C. *Inorg. Chem.* **2008**, *47*, 8583.

(33) Li, J.; Kathmann, S. M.; Schenter, G. K.; Gutowski, M. *J. Phys. Chem. C* **2007**, *111*, 3294.

(34) ADF 2009.01; SCM, Theoretical Chemistry, Vrije Universiteit: Amsterdam, The Netherlands ([www.scm.com](http://www.scm.com)).

(35) (a) Perdew, J. P.; Wang, Y. *Phys. Rev. B* **1986**, *33*, 8800. (b) Perdew, J. P.; Chevary, J. A.; Vosko, S. H.; Jackson, K. A.; Pederson, M.; Singh, D. J.; Fiolhais, C. *Phys. Rev. B* **1992**, *46*, 6671.

(36) Lenthe, E. V.; Baerends, E. J. *J. Comput. Chem.* **2003**, *24*, 1142.

(37) Henkelman, G.; Uberuaga, B. P.; Jónsson, H. *J. Chem. Phys.* **2000**, *113*, 9901.

(38) Stewart, J. J. P. et al. *MOPAC 5.09mm*; University of Minnesota: Minneapolis, 1999.

(39) Frisch, M. J.; Trucks, G. W.; Schlegel, H. B.; Scuseria, G. E.; Robb, M. A.; Cheeseman, J. R.; Zakrzewski, V. G.; Montgomery, J. A.; Stratmann, R. E.; Burant, J. C.; Dapprich, S.; Millam, J. M.; Daniels, A. D.; Kudin, K. N.; Strain, M. C.; Farkas, O.; Tomasi, J.; Barone, V.; Cossi, M.; Cammi, R.; Mennucci, B.; Pomelli, C.; Adamo, C.; Clifford, S.; Ochterski, J.; Petersson, G. A.; Ayala, P. Y.; Cui, Q.; Morokuma, K.; Malick, D. K.; Rabuck, A. D.; Raghavachari, K.; Foresman, J. B.; Cioslowski, J.; Ortiz, J. V.; Stefanov, B. B.; Liu, G.; Liashenko, A.; Piskorz, P.; Komaromi, I.; Gomperts, R.; Martin, R. L.; Fox, D. J.; Keith, T.; Al-Laham, M. A.; Peng, C. Y.; Nanayakkara, A.; Gonzalez, C.; Challacombe, M.; Gill, P. M. W.; Johnson, B. G.; Chen, W.; Wong, M. W.; Andres, J. L.; Head-Gordon, M.; Replogle, E. S.; Pople, J. A. *Gaussian 98*, revision A.1; Gaussian, Inc.: Pittsburgh, PA, 1998.

transition state geometries, the minimum energy paths connecting the reactants to products via the transition states were determined using the intrinsic reaction coordinate (IRC) approach.<sup>40,41</sup> The forward and backward reaction paths were optimized with step lengths ranging from 0.1 to 0.5 (amu)<sup>1/2</sup> bohr, adjusted according to the flatness of the potential energy surface. All the reported energies and geometries are from the ADF calculations unless specified otherwise.

Because of the N→B dative bonds, BNH<sub>x</sub> systems tend to have large charge transfer between the B- and N-containing groups, which could limit the accuracy of some DFT functionals. We therefore performed further DFT calculations with hybrid exchange-correlation functionals and *ab initio* wave function calculations on some of the structures obtained from the ADF PW91 calculations. These calculations were carried out at the levels of PW91, B3LYP, MP2, and CCSD(T) with 6-31++G(d,p) Gaussian basis sets and were accomplished by using NWChem 4.7.<sup>42</sup>

CPMD simulations were performed at  $T = 0, 200, 500, 1000, 2000, 3000, 4000,$  and  $5000$  K for the NH<sub>3</sub>BH<sub>3</sub> monomer, tetramer, and H(NH<sub>2</sub>BH<sub>2</sub>)<sub>n</sub>H oligomers ( $n = 2, 3, 4$ ) to explore reaction pathways and possible products of thermal decomposition.<sup>43</sup> The coiled structures we found previously were used as the starting structures for the CPMD simulations.<sup>33</sup> Simulated Annealing (SA) calculations and subsequent energy minimizations were carried out to determine the most stable structures and their energies. The oligomers were initially thermally equilibrated and then annealed with a time step of 5 au. Both simulation steps were carried out for 2.419 ps with a final temperature after annealing of less than 90 K. Similar CPMD simulations were performed for an ensemble of four NH<sub>3</sub>BH<sub>3</sub> molecules connected via intermolecular dihydrogen bonds to explore the intermolecular dehydrogenations.<sup>44</sup> This tetra-molecular system might provide useful information about the possible reaction mechanism in bulk crystalline NH<sub>3</sub>BH<sub>3</sub>.

These CPMD simulations were accomplished at the level of GGA using the PBE exchange-correlation functional<sup>45</sup> and were performed using the NWPW module of the plane-wave DFT method implemented in NWChem 4.7.<sup>42</sup> Hamann norm-conserving pseudopotentials were used for B, N, and H together with the plane-wave basis sets.<sup>46</sup> The supercell consists of a  $30 \times 30 \times 30$  bohr<sup>3</sup> simple cubic lattice and a  $64 \times 64 \times 64$  grid for discretization along lattice vector directions, which corresponds to a plane-wave cutoff energy of 22.459 hartree (611.1 eV). Test calculations show that such energy cutoff is sufficient for the systems calculated.

## Results and Discussion

It is envisaged that one of the thermal evolutions of the NH<sub>3</sub>BH<sub>3</sub> material proceeds through formation of H(NH<sub>2</sub>BH<sub>2</sub>)<sub>n</sub>H oligomers and their further dehydrogenation. Experimental work shows that oligomers are indeed formed in condensed phases;<sup>7,13,23,26</sup> however, there is little insight on

the mechanism of formation and dehydrogenation of the oligomers.<sup>16,47</sup> A few transition state calculations were performed for the dehydrogenation of the NH<sub>3</sub>BH<sub>3</sub> monomer<sup>48,49</sup> and dimer,<sup>33</sup> and for the dimerization of two aminoborane NH<sub>2</sub>BH<sub>2</sub> molecules.<sup>50</sup> Here we report on the formation and dehydrogenation mechanisms for the oligomers H(NH<sub>2</sub>BH<sub>2</sub>)<sub>n</sub>H ( $n = 1-4$ ). Various types of transition states have been investigated and several reactions pathways are explored. The results will be presented in six sections: (I) CPMD simulations to explore the potential intra- and intermolecular dehydrogenation products. (II) Transition states involving the B–N bond cleavage during dehydrogenation. (III) Transition states formed by H<sub>N</sub>→H<sub>B</sub> hydrogen transfer. (IV) Intermolecular dehydrogenation of NH<sub>3</sub>BH<sub>3</sub> molecules. (V) Formation mechanism of the oligomers. For convenience, we refer to the H<sub>3</sub>N- and the -BH<sub>3</sub> groups in H-(NH<sub>2</sub>BH<sub>2</sub>)<sub>n</sub>-H as the “head” and “tail”, respectively, while H<sub>N</sub> and H<sub>B</sub> denote, respectively, a protic ( $\delta^+$ ) hydrogen H<sub>N</sub> bonded to a N atom and the a hydridic ( $\delta^-$ ) hydrogen H<sub>B</sub> bonded to a B atom.

**I. CPMD Simulations for H(NH<sub>2</sub>BH<sub>2</sub>)<sub>n</sub>H ( $n = 1, 2, 3, 4$ ) and (NH<sub>3</sub>BH<sub>3</sub>)<sub>4</sub>.** CPMD simulations of the H(NH<sub>2</sub>BH<sub>2</sub>)<sub>n</sub>H ( $n = 1, 2, 3, 4$ ) oligomers and a cluster of four NH<sub>3</sub>BH<sub>3</sub> molecules were accomplished at a variety of temperatures to provide information of the intra- and intermolecular reaction dynamics. These calculations did not aim at providing dynamics of the systems at the actual reaction temperature because of the very short simulation time. Instead the goal was to provide information on the possible intra- and intermolecular thermal decomposition channels. Therefore the reported temperatures for formation of new products are relatively high as resulting from the short-time simulations. The actual reactions might be studied at much lower temperature if significantly longer simulation times on the nanosecond scale were practical. However, the CPMD simulation times required to unravel decomposition pathways at standard temperatures would be prohibitively long and some accelerated dynamics approaches would be needed.<sup>51–53</sup>

The potential reaction products from the CPMD simulations of the (NH<sub>3</sub>BH<sub>3</sub>)<sub>n</sub> ( $n = 1, 4$ ) clusters and the H(NH<sub>2</sub>BH<sub>2</sub>)<sub>n</sub>H ( $n = 1, 2, 3, 4$ ) oligomers at  $T = 1000, 2000, 3000, 4000,$  and  $5000$  K are listed in Tables 1 and 2, respectively. The optimized geometries from the CPMD final structures at these temperatures are shown in Supporting Information, Figures S1 and S2. The simulations for other temperatures ( $T = 200, 500,$  and  $1250$  K) were performed to investigate the dynamics of the systems at relatively lower temperature, and the results are not shown for brevity.

From Table 1, with the picosecond scale simulations, the NH<sub>3</sub>BH<sub>3</sub> molecule is stable at low-temperature, but at

(40) Ishida, K.; Morokuma, K.; Komornicki, A. *J. Chem. Phys.* **1977**, *66*, 2153.

(41) Deng, L.; Ziegler, T.; Fan, L. Y. *J. Chem. Phys.* **1993**, *99*, 3823–3835. Deng, L.; Ziegler, T. *Int. J. Quantum Chem.* **1994**, *52*, 731.

(42) Aprà, E.; Windus, T. L. et al. *NWChem, A Computational Chemistry Package for Parallel Computers*, Version 4.7; Pacific Northwest National Laboratory: Richland, WA, 2005; 99352–0999.

(43) Car, R.; Parrinello, M. *Phys. Rev. Lett.* **1985**, *55*, 2471.

(44) Crabtree, R. H. *Science* **1998**, *282*, 2000.

(45) Perdew, J. P.; Burke, K.; Ernzerhof, M. *Phys. Rev. Lett.* **1996**, *77*, 3865.

(46) Hamann, D. R. *Phys. Rev. B* **1989**, *40*, 2980.

(47) Shaw, W. J.; Bowden, M. B.; Karkamkar, A.; Howard, C. J.; Heldebrandt, D. J.; Bowden, M.; Hess, N. J.; Linehan, J. C.; Autrey, T. *Environ. Eng. Sci.* **2010**, *3*, 796.

(48) Li, Q. S.; Zhang, J.; Zhang, S. *Chem. Phys. Lett.* **2005**, *404*, 100.

(49) Nguyen, M. T.; Nguyen, V. S.; Matus, M. H.; Gopakumar, G.; Dixon, D. A. *J. Phys. Chem. A* **2007**, *111*, 679.

(50) Gilbert, T. M. *Organometallics* **1998**, *17*, 5513.

(51) Chandler, D. Finding Transition Pathways: Throwing Ropes Over Rough Mountain Passes, in the Dark. In *Computer Simulation of Rare Events and Dynamics of Classical and Quantum Condensed-Phase Systems -- Classical and Quantum Dynamics in Condensed Phase Simulations*; Berne, B. J., Ciccotti, G., Coker, D. F., Eds.; World Scientific: Singapore, 1998; pp 51–66.

(52) Sorensen, M. R.; Voter, A. F. *J. Chem. Phys.* **2000**, *112*, 9599.

(53) Laio, A.; Parrinello, M. *Proc. Natl. Acad. Sci. U.S.A.* **2002**, *99*, 12562.



**Table 1.** Identified Decomposition Products in CPMD Simulations of the Ammonia Borane Monomer and Tetramer  $(\text{NH}_3\text{BH}_3)_n$  Where  $n = 1$  and 4

$T$ (K)	decomposition products
$n = 1$	
5000	$\text{H}_2\text{N}=\text{BH}_2 + \text{H}_2$
4000	$\text{NH}_3 + \text{BH}_3$
3000	$\text{NH}_3 + \text{BH}_3$
2000	$\text{NH}_3 + \text{BH}_3$
1000	$\text{NH}_3\text{BH}_3$
0	$\text{NH}_3\text{BH}_3$
$n = 4$	
5000	$2\text{H}_2\text{N}=\text{BH}_2 + 2\text{NH}_3 + \text{H}_2\text{B}(\mu\text{-H})_2\text{BH}_2 + 2\text{H}_2$
4000	$\bullet\text{NH}_2\text{BH}_3 + \text{NH}_3\text{H}_2\text{B}\bullet + 2\text{NH}_3 + \text{H}_2\text{B}(\mu\text{-H})_2\text{BH}_2 + \text{H}_2$
3000	$\text{NH}_3\text{BH}_3 + 2\text{NH}_3 + \text{BH}_3 + \text{H}_2\text{B}(\mu\text{-H})(\mu\text{-NH}_2)\text{BH}_2 + \text{H}_2$
2000	$\text{NH}_3 + \text{H}_3\text{NBH}_2^+(\text{BH}_4)^- + \text{NH}_3\text{BH}_3 + \text{NH}_2=\text{BH}_2 + \text{H}_2$
1000	$4\text{NH}_3\text{BH}_3$
0	$4\text{NH}_3\text{BH}_3$

**Table 2.** Identified Decomposition Products in CPMD Simulations of the  $\text{H}(\text{BH}_2\text{NH}_2)_n\text{H}$  ( $n = 2, 3, 4$ ) Oligomers

$T$ (K)	decomposition products
$n = 2$	
5000	$\text{NH}_3 + \text{BH}_3 + \text{H}_2\text{N}=\text{BH}_2$
4000	$\text{HN}=\text{BH} + \text{NH}_3 + \text{BH}_3 + \text{H}_2$
3000	$\text{H}_2\text{N}=\text{BH}_2 + \text{NH}_3 + \text{BH}_3$
2000	$\text{H}_2\text{N}-\text{BH}(\mu\text{-H})_2-\text{BH}_2 + \text{NH}_3$
1000	$\text{NH}_3\text{BH}_2-\text{NH}_2\text{BH}_3$
0	$\text{NH}_3\text{BH}_2-\text{NH}_2\text{BH}_3$
$n = 3$	
5000	$\text{H}_2\text{N}=\text{BH}_2 + \text{NH}_3 + \text{H}_2\text{B}-\text{N}=\text{BH} + 2\text{H}_2$
4000	$\text{H}_2\text{N}=\text{BH}_2 + \text{BH}_3 + \text{H}_2\text{N}-\text{BH}-\text{NH}_2 + \text{H}_2$
3000	$\text{NH}_2\text{BH}_2 + \text{HN}=\text{BH} + \text{NH}_3 + \text{BH}_3 + \text{H}_2$
2000	$\text{H}_2\text{N}-\text{BH}(\mu\text{-H})_2-\text{BH}_2 + \text{H}_2\text{N}=\text{BH}_2 + \text{NH}_3$
1000	$\text{NH}_3\text{BH}_2-\text{NH}_2\text{BH}_2-\text{NH}_2\text{BH}_3$
0	$\text{NH}_3\text{BH}_2-\text{NH}_2\text{BH}_2-\text{NH}_2\text{BH}_3$
$n = 4$	
5000	$\text{H}_2\text{N}=\text{BH}_2 + \text{H}_2\text{B}(\mu\text{-H})(\mu\text{-NH})\text{BH} + \text{H}_2\text{N}-\text{BH}-\text{NH}_2 + 2\text{H}_2$
4000	$\text{H}_3\text{N}-\text{BH}_3 + 2\text{H}_2\text{N}=\text{BH}_2 + \text{H}_2\text{N}-\text{B} + \text{H}_2$
3000	$2\text{H}_2\text{N}=\text{BH}_2 + \text{NH}_3 + \text{H}_2\text{B}(\mu\text{-H})(\mu\text{-NH}_2)\text{BH}_2$
2000	$3\text{H}_2\text{N}=\text{BH}_2 + \text{NH}_3 + \text{BH}_3$
1000	$\text{NH}_3\text{BH}_2-\text{NH}_2\text{BH}_2-\text{NH}_2\text{BH}_2-\text{NH}_2\text{BH}_3$
0	$\text{NH}_3\text{BH}_2-\text{NH}_2\text{BH}_2-\text{NH}_2\text{BH}_2-\text{NH}_2\text{BH}_3$

medium simulation temperatures there occurs a B–N bond cleavage to generate  $\text{NH}_3$  (pyramidal) and  $\text{BH}_3$  (planar). Above 4000 K the  $\text{NH}_2\text{BH}_2$  molecules are formed with the release of  $\text{H}_2$ . The same two types of possible reactions will be discussed later in the context of transition states searches. It is interesting to note that with the increase of simulation temperature the B–N bond cleavage occurs *before* the release of  $\text{H}_2$  and the formation of  $\text{NH}_2\text{BH}_2$ . This result is not unexpected given that the B–N dative bond is relatively weak when comparing with normal covalent bonds.<sup>54,11</sup> Indeed a recent kinetic analysis shows that the reaction of the B–N bond cleavage process is 10 orders of magnitude faster than the dihydrogen release process at 1 atm and 298 K.<sup>49</sup>

For the cluster of four  $\text{NH}_3\text{BH}_3$  molecules, the reactions are more complex as both the intra- and intermolecular transformations are possible. Above 1000 K one observes the B–N bond cleavage with the resulting  $\text{BH}_3$

reacting with the remaining  $\text{NH}_3\text{BH}_3$  and forming  $\text{H}_3\text{N}-\text{BH}_2^+(\text{BH}_4)^-$ , as well as formation of  $\text{NH}_2\text{BH}_2$  with the release of  $\text{H}_2$ . At higher temperatures one observes formation of diborane  $\text{H}_2\text{B}(\mu\text{-H})_2\text{BH}_2$  and  $\mu$ -aminodiborane (ADB)  $\text{H}_2\text{B}(\mu\text{-H})(\mu\text{-NH}_2)\text{BH}_2$ . The latter might be viewed as a diborane with a  $\mu\text{-H}$  replaced with  $\mu\text{-NH}_2$ . One even observes formation of  $\bullet\text{NH}_2\text{BH}_3$  and  $\text{NH}_3\text{H}_2\text{B}\bullet$  radicals at elevated temperatures. These CPMD calculations at different simulation temperatures are informative: many of the species from the simulations were previously identified in experiments. For example, the ADB complex was seen in previous experiments,<sup>55</sup> and has been shown to be a minor product accompanying the main reaction pathway.<sup>14</sup> The vapors above the solid  $\text{NH}_3\text{BH}_3$  at room temperature are found to contain molecules of  $\text{NH}_3\text{BH}_3$ ,  $\text{NH}_2\text{BH}_2$ , and  $\text{H}_2\text{B}(\mu\text{-H})_2\text{BH}_2$ ,<sup>17</sup> which are all predicted to form in the CPMD simulations (Table 1, Supporting Information, Figure S1). Of particular interest in the 2000 K CPMD simulation of the cluster of four  $\text{NH}_3\text{BH}_3$  molecules is the formation of another intermediate  $\text{H}_3\text{N}-\text{BH}_2^+(\text{BH}_4)^-$ . This intermediate can be formed by the attachment of  $\text{BH}_3$  to the  $\text{NH}_3\text{BH}_3$ . Upon coordination of an additional  $\text{NH}_3$  to the electron-deficient  $\text{BH}_2^+$  end-group this intermediate forms the diammoniate of diborane (DADB) complex,  $(\text{H}_3\text{N})_2\text{BH}_2^+(\text{BH}_4)^-$ , a well-known and common species in ammonia borane chemistry.<sup>56</sup>

The possible products from the CPMD simulations on the oligomers (Table 2) are similar to those listed in Table 1, and the species formed in the simulations for  $n = 3$  and  $n = 4$  are also partly similar to those for  $n = 2$ . Consistent with our previous results, the  $n = 2$  molecule has a coiled structure at 0 K, in which the  $-\text{NH}_3$  head and the  $-\text{BH}_3$  tail are bound through dihydrogen bonds.<sup>33</sup> The dihydrogen bonds in the coiled structures are very short, only 1.43 Å, with a head–tail N–B distance of  $\sim 3.03$  Å. With the increase of simulation temperature from 200 to 1500 K, the dihydrogen bonds are gradually weakened and the  $\text{NH}_3$  and  $\text{BH}_3$  groups start to rotate freely. Starting from around 2000 K, at least one N–B bond is ruptured, and the molecular products include the  $\text{H}_2$ , pyramidal  $\text{NH}_3$ , and planar  $\text{BH}_3$  molecules, as well as other products/intermediates seen in Table 1, including  $\text{NH}_2\text{BH}_2$  and ADB (at  $T = 3000$  K, and  $n = 4$ ). The formation of  $\text{BH}_3$  is particularly interesting because it can trigger an acid-initiated hydrogen release, as shown previously.<sup>57</sup>

By comparing with those species listed in Table 1, the new species formed in some of these processes are  $\text{H}_2\text{N}-\text{BH}(\mu\text{-H})_2-\text{BH}_2$  ( $n = 2$ , 2000 K;  $n = 3$ , 2000 K),  $\text{H}_2\text{B}-\text{N}=\text{BH}$  ( $n = 3$ , 5000 K),  $\text{H}_2\text{N}-\text{BH}-\text{NH}_2$  ( $n = 3$ , 4000 K;  $n = 4$ , 5000 K),  $\text{H}_2\text{B}(\mu\text{-H})(\mu\text{-NH})\text{BH}$  ( $n = 4$ , 5000 K), and even  $\text{HN}=\text{BH}$  ( $n = 2$ , 4000 K) and  $\text{H}_2\text{N}-\text{B}$  ( $n = 4$ , 4000 K). The  $\text{H}_2\text{N}-\text{BH}(\mu\text{-H})_2-\text{BH}_2$  molecule is an isomer of the ADB molecule, and can be viewed as a dihydrogen release product from the  $\text{H}_3\text{N}-\text{BH}_2^+(\text{BH}_4)^-$  intermediate, which is a precursor to the formation of DADB (see above). The  $\text{H}_2\text{B}(\mu\text{-H})(\mu\text{-NH})\text{BH}$  molecule is a product of dihydrogen release from ADB. Other species

(55) Schwartz, L. D.; Keller, P. C. *J. Am. Chem. Soc.* **1972**, *94*, 3015.(56) Parry, R. W. *J. Chem. Educ.* **1997**, *74*, 512.(57) Stephens, F. H.; Baker, R. T.; Matus, M. H.; Grant, D. J.; Dixon, D. A. *Angew. Chem., Int. Ed.* **2007**, *46*, 746.(54) Grant, D. J.; Dixon, D. A. *J. Phys. Chem. A* **2006**, *110*, 12955.

**Table 3.** Structures and Energies of Reactants (R), Transition States (TS), and Products (P) of B–N Bond Cleavage Reactions of  $\text{H}(\text{NH}_2\text{BH}_2)_n\text{H}$  ( $n = 1, 2, 3$ )<sup>a</sup>

R	$\Delta E_R$	TS	$\Delta E_{TS}$	$\nu$	P	$\Delta E_P$
<b>n=1</b>						
	0	Barrierless	-	-		29.80
<b>n=2</b>						
	0		25.16	380i		12.28
	0		8.58	370i		-16.66
<b>n=3</b>						
	0		40.89	193i		18.22

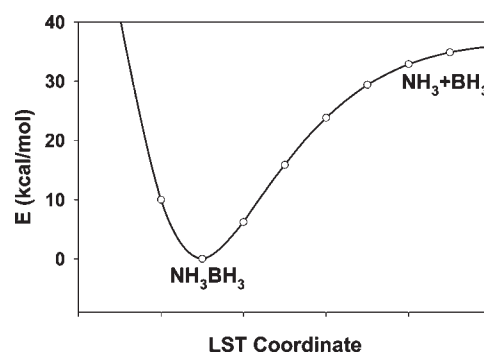
<sup>a</sup>All the energies (in kcal/mol) are calculated using ADF PW91/TZ2P and are relative to the energies of the reactants. Imaginary frequencies of the transition states are listed to show the breadth of the activation barriers. The color code: B, orange; N, blue; H, cyan; dihydrogen H, yellow.

with multiple BN bonds are also possible when  $\text{H}(\text{NH}_2\text{BH}_2)_n\text{H}$  and clusters of  $\text{NH}_3\text{BH}_3$  are heated to very high temperatures.

In summary, the CPMD simulations have shown that at low temperatures two types of reactions occur: (i) the B–N bond cleavage to form  $\text{BH}_3 + \text{NH}_3$ , and (ii) the formation of  $\text{NH}_2\text{BH}_2$  with intramolecular  $\text{H}_2$  release. At higher temperatures, both intra- and intermolecular dehydrogenation occur, forming DADB precursors and the complexes with the BN double or even triple bonds. Many of these molecular species are found as products or intermediates from our transition state and IRC calculations (see below).

**II. Intramolecular Dehydrogenation Involving N–B Bond Cleavage in  $\text{H}(\text{NH}_2\text{BH}_2)_n\text{H}$  ( $n = 1-3$ ).** In this section we will present the computational results of transition state searches and IRC calculations on the B–N bond cleavage and hydrogen-transfer processes. These two kinds of processes both involve only intramolecular reactions.

**N–B Bond Cleavage in  $\text{H}(\text{NH}_2\text{BH}_2)_n\text{H}$  ( $n = 1-3$ ).** The structures and energies of the reactants, transition states, and products of decomposition steps involving N–B bond cleavage and dehydrogenation in  $\text{H}(\text{NH}_2\text{BH}_2)_n\text{H}$  ( $n = 1-3$ ) are listed in Table 3. For the  $\text{NH}_3\text{BH}_3$  monomer, the homolytic B–N cleavage is barrierless as only the dative bond is elongated during the bond breaking. The endothermicity of this step is illustrated in Figure 1 by the potential energy curve of B–N bond cleavage. The energies are determined by linear synchronous transit (LST) calculations of the  $\text{NH}_3\text{BH}_3$  molecule from its staggered global minimum structure to a supermolecule



**Figure 1.** Calculated linear synchronous transit (LST) potential energy curve (in kcal/mol) of the B–N bond cleavage in  $\text{NH}_3\text{BH}_3$  (the maximum LST coordinate corresponding to B–N = 7 Å).

structure where the  $\text{NH}_3$  and  $\text{BH}_3$  are 7 Å away from each other. While the zero-point energy (ZPE) corrections are not included in this LST curve, the process of the B–N bond cleavage is endothermic with a ZPE-corrected decomposition energy of 28.7 kcal/mol at the PW91 level. This binding energy of  $\text{NH}_3$  and  $\text{BH}_3$  is close to the CCSD(T) value (25.9 kcal/mol)<sup>11,49</sup> and the estimated experimental result (31.1 kcal/mol).<sup>58</sup> It suggests that the decomposition reaction  $\text{NH}_3\text{BH}_3 \rightarrow \text{NH}_3 + \text{BH}_3$  is possible at elevated reaction temperatures, consistent with the CPMD simulations for  $\text{NH}_3\text{BH}_3$  at medium temperatures.

The N–B bond cleavage of  $\text{NH}_3\text{BH}_3$  molecules is consistent with previous experiments using pyridine solutions

(58) Haaland, A. *Angew. Chem., Int. Ed.* **1989**, 28, 992.

where  $\text{NH}_3\text{BH}_3$  is quantitatively converted to pyridineborane ( $\text{PyBH}_3$ ) with ammonia release into the gas phase.<sup>14</sup> The decomposition of  $\text{NH}_3\text{BH}_3$  via N–B bond cleavage is, in general, undesirable for fuel cell applications. However, the release of  $\text{NH}_3$  and  $\text{BH}_3$  (or its dimer  $\text{B}_2\text{H}_6$ ) to the environment is very improbable under thermal decomposition. In fact, because  $\text{NH}_3$  is a strong electron donor and the electron-deficient  $\text{BH}_3$  has a large hydride affinity, these species are highly reactive and can easily be consumed by subsequent reactions with the remaining  $\text{NH}_3\text{BH}_3$  molecules or the  $\text{H}(\text{NH}_2\text{BH}_2)_n\text{H}$  oligomers. Indeed in experiments on the decomposition reactions of  $\text{NH}_3\text{BH}_3$  materials only trace amounts of ammonia and diborane are detected, indicating that if they are formed they may be rapidly consumed.<sup>8,19,59</sup> Moreover, recent theoretical studies show that  $\text{BH}_3$  in fact serves as an efficient bifunctional acid–base catalyst for dihydrogen release reactions.<sup>49</sup> Therefore, the B–N bond cleavage in  $\text{NH}_3\text{BH}_3$  does not lead to dihydrogen release, but provides reactive species that catalyze the subsequent dehydrogenation reactions.

For  $n = 2$ , we found a transition state  $\text{NH}_2\text{BH}_2\text{NH}_2\text{-BH}_2(\eta^2\text{-H}_2)$  (**2-TS1**) that has an imaginary frequency of  $380i \text{ cm}^{-1}$  and an activation barrier of 25.2 kcal/mol, see Table 3. **2-TS1** is formed by migrating one hydrogen atom from the  $\text{NH}_3$  head to the electron-deficient  $\text{BH}_3$  tail to form a dihydrogen molecule being side-on bonded to the boron atom in the tail. We will see throughout this work that this type of *dihydrogen interaction* with boron plays a significant role in stabilizing various transition states. The dihydrogen interaction with B can be viewed as the hydrogen-transfer from N to B, where the  $\text{H}_\text{N}$  and  $\text{H}_\text{B}$  atoms are already weakly bound by a dihydrogen bond in the coiled structure of the reactant. The stability of the dihydrogen interaction with B is not unexpected given that the B center is electron-deficient such that formation of a  $\sigma$ -complex with a  $\text{R-BH}_2(\eta^2\text{-H}_2)$  moiety is energetically feasible without violating the classic *octet rule*. Indeed stable  $\text{BH}_3(\eta^2\text{-H}_2)$  molecules and  $\text{BNH}_x$  dihydrogen intermediates are found in our calculations and also in previous research on boron systems.<sup>60,61</sup>

In **2-TS1**, the nascent dehydrocoupled  $\text{H}_2$  molecule ( $\text{H-H} = 0.80 \text{ \AA}$ ) lies in the same plane as the  $\text{BN}\cdots\text{BN}$  skeleton, and the two H atoms are  $1.66 \text{ \AA}$  and  $1.99 \text{ \AA}$  from the terminal B, and  $1.87 \text{ \AA}$  and  $2.66 \text{ \AA}$  from the terminal N. As the head and tail are only loosely bonded by the activated  $\text{H}_2$  molecule, they form partial B–N double bonds to comply with the octet rule. Indeed, our calculations show that in **2-TS1** the terminal B–N distances are quite short ( $1.44 \text{ \AA}$  and  $1.46 \text{ \AA}$ ), whereas the binding of the central B–N bond is weakened and elongated to  $2.13 \text{ \AA}$ . The transition state structure can thus be viewed as  $\text{NH}_2\text{BH}_2(\eta^2\text{-H}_2)$  weakly bound with another  $\text{NH}_2\text{BH}_2$  through the central connecting part.

Consistent with this notion, the IRC calculations reveal that the forward reaction from **2-TS1** leads to the formation of two  $\text{NH}_2\text{BH}_2$  plus  $\text{H}_2$ , and the reaction is endothermic

by 12.3 kcal/mol from the coiled  $n = 2$  structure. The two  $\text{NH}_2\text{BH}_2$  intermediate molecules can easily dimerize to form a cyclic  $\text{c}(\text{NH}_2\text{BH}_2)_2$  molecule, cyclodiaminoborane (CDB) via a transition state **2-TS2**; the barrier height of **2-TS2** is only 8.6 kcal/mol at the PW91 level, which is consistent with other calculations, 8.5 kcal/mol at MP4, and 10.7 kcal/mol with B3LYP.<sup>50</sup> Therefore, the formation of **2-TS1** is a rate-determining step for the overall cyclization reaction  $\text{H}(\text{NH}_2\text{BH}_2)_2\text{H} \rightarrow \text{c}(\text{NH}_2\text{BH}_2)_2 + \text{H}_2$ . The dimerization of  $\text{NH}_2\text{BH}_2$  to form CDB is exothermic by  $-16.7 \text{ kcal/mol}$ , so that the overall reaction from  $\text{H}(\text{NH}_2\text{BH}_2)_2\text{H}$  is moderately exothermic ( $-4.4 \text{ kcal/mol}$ ).

For the  $n = 3$  oligomer, the transition state **3-TS1** (see Table 3) is formed when a hydrogen transfers from the head to the tail. While **3-TS1** is clearly analogous to **2-TS1**, the activated  $\text{H}_2$  molecule ( $\text{H-H} = 0.77 \text{ \AA}$ ) is bound more weakly to the head and the tail than in **2-TS1**, with the shortest  $\text{H}_2\cdots\text{B}$  and  $\text{H}_2\cdots\text{N}$  distances close to  $2.33 \text{ \AA}$ . Consequently, the PW91 activation barrier of 40.9 kcal/mol is larger than that of **2-TS1**. The **3-TS1** structure can be viewed as  $\text{H}_2$  bound to three weakly bonded  $\text{NH}_2\text{BH}_2$  molecules, as the N–B distances alternate ( $1.51 \text{ \AA}$ ,  $1.72 \text{ \AA}$ ,  $1.52 \text{ \AA}$ ,  $1.85 \text{ \AA}$ ,  $1.46 \text{ \AA}$ ) from the head to the tail. Our IRC calculations show that the back reaction via **3-TS1** forms the coiled structure for  $n = 3$ , in which all the B–N distances lie between  $1.58 \text{ \AA} \sim 1.63 \text{ \AA}$ . In the forward reaction, the transition state **3-TS1** decomposes into  $\text{H}_2$ ,  $\text{NH}_2\text{BH}_2$ , and a unique intermediate  $\text{H}_2\text{B}(\mu\text{-H})(\mu\text{-NH}_2)\text{-BH-NH}_2$  with all-real frequencies, in which a  $\mu\text{-H}$  and  $\mu\text{-NH}_2$  bridge the two B atoms via three-center two-electron ( $3c2e$ ) bonds. This intermediate is an amino-substituted derivative of the  $\mu$ -aminodiborane identified in our preceding CPMD simulations of thermal decomposition and can be viewed as a product of releasing two  $\text{H}_2$  molecules from the diammoniate of diborane complex  $[(\text{NH}_3)_2\text{-}(\text{BH}_2)]^+(\text{BH}_4)^-$  (DADB). The reaction through **3-TS1** is endothermic by 18.2 kcal/mol. However, the product  $\text{H}_2\text{B}(\mu\text{-H})(\mu\text{-NH}_2)\text{-BH-NH}_2$  can isomerize to the much more stable  $\text{c}(\text{NH}_2\text{BH}_2)_2$  molecule releasing 8.6 kcal/mol in energy, while two  $\text{H}_2\text{NBH}_2$  molecules can also be transformed to  $\text{c}(\text{NH}_2\text{BH}_2)_2$  molecule via **2-TS2**, releasing 16.7 kcal/mol in energy.

The transition states listed in Table 3 all lead to the B–N bond cleavages in the oligomers. The decomposition of the  $\text{NH}_3\text{BH}_3$  monomer is endothermic in the gas-phase, while the overall reactions of  $n = 2$  are exothermic and the reaction for  $n = 3$  to form  $\text{c}(\text{NH}_2\text{BH}_2)_2$  molecules is nearly thermoneutral. The decomposition of the  $n = 2$  oligomer has a lower relative activation barrier of 25.2 kcal/mol, while the rate-determining step of the  $n = 3$  oligomer has a barrier being *higher* by 15.7 kcal/mol. Without catalysts, these reactions will only occur when temperatures are raised high enough to activate the reactants. The imaginary frequencies for **2-TS1** and **3-TS1** are rather small, suggesting that the widths of the barriers might be too large to allow for significant tunneling.

**III. Dehydrogenation through Hydrogen-Transfer Transition States in  $\text{H}(\text{NH}_2\text{BH}_2)_n\text{H}$  ( $n = 1\text{--}3$ ).** As shown from the previous CPMD simulations, aminoborane  $\text{NH}_2\text{BH}_2$  is the common product of dehydrogenation of the  $\text{NH}_3\text{BH}_3$  monomer,  $(\text{NH}_3\text{BH}_3)_n$  clusters, and the  $\text{H}(\text{NH}_2\text{BH}_2)_n\text{H}$  ( $n = 2, 3, 4$ ) oligomers. The formation of  $\text{NH}_2\text{BH}_2$  via

(59) Kuznesof, P. M.; Shriver, D. F.; Stafford, F. E. *J. Am. Chem. Soc.* **1968**, *90*, 2257.

(60) Rasul, G.; Prakash, G. K. S.; Olah, G. A. *Proc. Natl. Acad. Sci. U.S.A.* **1998**, *95*, 7257.

(61) (a) Welch, G. C.; Juan, R. R. S.; Masuda, J. D.; Stephan, D. W. *Science* **2006**, *314*, 1124. (b) Kubas, G. J. *Science* **2006**, *314*, 1096.



**Table 4.** Summary of Reactants (R), Transitions States (TS), and Products (P) of Dehydrocoupling Reactions via Hydrogen-Transfer Transition States<sup>a</sup>

oligomer	R	TS	$\Delta E_{\text{TS}}$	$\nu_{\text{TS}}$	P	$\Delta E_{\text{P}}$
n=1			32.2 <sup>b</sup>	1269i		-0.3
n=2			40.4	1292i		+8.4
n=2			59.1	1401i		+23.5
n=2			37.3	1210i		+6.9
n=3			49.4	1086i		-9.7

<sup>a</sup> All the energies (in kcal/mol) are calculated using ADF PW91/TZ2P and are relative to the energies of the reactants. Imaginary frequencies of the transition states are listed. The color code: B, yellow; N, blue; H, cyan; dihydrogen H, orange. <sup>b</sup> The IRC finds the eclipsed conformer, which is 1.9 kcal/mol above the staggered global minimum structure of NH<sub>3</sub>BH<sub>3</sub>.

dehydrogenation of NH<sub>3</sub>BH<sub>3</sub> is consistent with previous experimental results for thermal decomposition of NH<sub>3</sub>BH<sub>3</sub>, where the formation of NH<sub>2</sub>BH<sub>2</sub> accompanies the first hydrogen-loss step.<sup>17,22,13</sup> Table 4 lists the structures and energies of the reactants, transition states, and products of the dehydrogenation reactions involving hydrogen-transfer from the head to the tail and across the chain for  $n = 1-3$ .

The hydrogen-transfer transition state of the NH<sub>3</sub>BH<sub>3</sub> monomer has been well studied in previous works.<sup>48,49</sup> Briefly, the NH<sub>3</sub>BH<sub>3</sub> monomer needs to rotate from its staggered global minimum structure to the eclipsed conformer, which requires only 1.9 kcal/mol energy from our PW91 calculations. The latter can form a transition state **1-TS2** through the H-N bending mode to transfer a hydrogen atom from NH<sub>3</sub> to BH<sub>3</sub>. The fact that the hydrogen-transfer is from N to B is consistent with the tendency to form the R-BH<sub>2</sub>( $\eta^2$ -H<sub>2</sub>) moiety via the dihydrogen interaction at B atom, as we discussed earlier for the B-N cleavage decomposition of the  $n = 2$  oligomer. The calculated PW91 activation barrier of **1-TS2** is 34.1 (or 32.2) kcal/mol with respect to the staggered (or eclipsed) structure, which is fairly close to the previous B3LYP value (34.6 kcal/mol) and the CBS/QB3 value (32.6 kcal/mol), but is slightly lower than the CCSD(T)/CBS

result (36.4 kcal/mol).<sup>48,49</sup> The reaction is slightly exothermic, consistent with other calculations.<sup>11,48,49,62</sup> The calculated imaginary frequency of **1-TS2** is 1269i cm<sup>-1</sup>, indicating the possibility that the hydrogen-transfer transition state of the monomer might be subject to large tunneling effects.

For  $n = 2$ , the hydrogen-transfer between the head and the tail leads to the B-N bond cleavage via **2-TS1**, as discussed in the previous section. We also investigated another dehydrogenation channel involving a hydrogen-transfer from N to neighboring B across the chain with the results listed in Table 4. The hydrogen-transfer transition states from B to N are not evaluated in detail because they would involve transferring a hydrogen atom from the electron-deficient center to the electron-rich center and are expected to be high in energy. Indeed one of our calculations located a hydrogen-transfer transition state from B to N, which is some 70 kcal/mol higher than the N to B transition state **2-TS1** and thus will not be considered here. Our calculations show that the local structures of all the hydrogen-transfer transition states are similar to that of NH<sub>3</sub>BH<sub>3</sub> with the DHI moiety R-BH<sub>2</sub>( $\eta^2$ -H<sub>2</sub>). The IRC calculations show that starting from the coiled  $n = 2$  structure these transition states all lead to H<sub>2</sub> release and formation of a B=N bond. The activation barriers are 40.4 kcal/mol for a hydrogen-transfer from the head N to

**Table 5.** DFT and *ab initio* Energies for the Reactions of  $\text{H}-(\text{NH}_2\text{BH}_2)_n-\text{H} \rightarrow (\text{NH}_2\text{BH}_2)_n + \text{H}_2$  ( $n = 1, 2, 3, 4$ )<sup>a</sup>

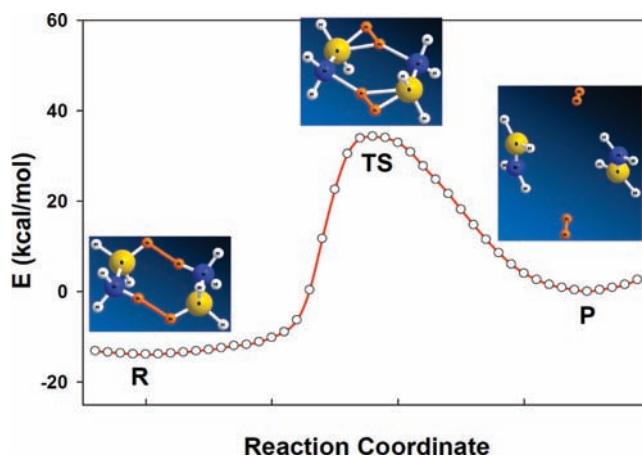
	PW91	B3LYP	MP2	CCSD(T)
$n = 1$	-0.3	-1.96	-0.91	-0.79
$n = 2$	-4.4	-2.89	-3.75	-2.97
$n = 3$	-9.7	-9.60	-12.14	-11.28
$n = 4$	-2.1	-4.74	-8.40	-7.48

<sup>a</sup> Used ADF PW91/TZ2P and NWChem B3LYP, MP2, and CCSD(T) with 6-31++G(d,p) basis sets. All the reaction energies are in kcal/mol. Cyclic products are formed for  $n \geq 2$ . The B3LYP and MP2 geometries are optimized, and the CCSD(T) energies are calculated at the optimized MP2 geometries.

its neighboring B in the chain, 59.1 kcal/mol for a hydrogen transfer in the middle B–N unit, and 37.3 kcal/mol for a hydrogen transfer from the neighboring N to the tail B, indicating that formation of the DHI transition state is more demanding in the central part than in the head or tail parts. However, the head-to-tail hydrogen transfer transition state **2-TS1** is energetically more favored than for any of the neighboring hydrogen transfers along the chain.

For  $n = 3$ , we find a transition state **3-TS2** that requires an activation barrier of 49.4 kcal/mol from the coiled structure identified in our previous work.<sup>33</sup> Interestingly, the dehydrocoupling along this reaction channel directly leads to the cyclic product cyclotriborazane (CTB). The dehydrogenation reaction is exothermic by 9.7 kcal/mol at the level of PW91 calculations. The one-step dehydrogenation, however, has a much higher activation barrier than **3-TS1**, which leads to a B–N bond cleavage. All these hydrogen-transfer activation barriers are larger than those involving the B–N bond cleavage, making them less favored kinetically. During the transition state search, we also find other DHI intermediates that may also contribute to the chemistry of ammonia borane. The role of these dihydrogen intermediates for  $n = 3$  and higher oligomers deserves further investigation.

The transition state calculations have provided important information about the possible pathways of dehydrogenation of ammonia borane and the oligomers. Inasmuch as DFT methods could have huge errors in calculating the energies of boron systems,<sup>63</sup> it is important to make certain that the energetics we calculated using the pure PW91 generalized gradient approach so far are reliable, particularly because the highly polarized  $\text{N} \rightarrow \text{B}$  dative bonds are involved. Table 5 lists the calculated energy of dehydrogenation for  $\text{H}-(\text{NH}_2\text{BH}_2)_n-\text{H} \rightarrow (\text{NH}_2\text{BH}_2)_n + \text{H}_2$  using GGA PW91 functional, the B3LYP hybrid functional, and MP2 and CCSD(T) *ab initio* methods, where cyclic products are formed for  $n \geq 2$ . Clearly, our PW91 results are fairly close to the hybrid DFT and *ab initio* results, and are consistent with previous CCSD(T) calculations.<sup>64</sup> In other words, the DFT methods are accurate within a few kcal/mol in evaluating the energetics, albeit underestimating the reaction energies compared with the MP2 and CCSD(T) results. The most interesting conclusion from these reaction energies is that the reaction is more thermoneutral for  $n = 1, 2$ , or 4 than for  $n = 3$ . The enhanced exothermicity for  $n = 3$  is consi-



**Figure 2.** Structures of the reactant, transition-state, and product, and IRC potential energy curve (in kcal/mol) of the intermolecular dehydrocoupling of two  $\text{NH}_3\text{BH}_3$  molecules (Color code: N, blue; B, yellow; H, cyan; dihydrogen H, orange).

istent with the facile formation of borazine,  $c\text{-(NHBH)}_3$ , among molecular species resulting from the thermolysis of  $\text{NH}_3\text{BH}_3$ .<sup>8</sup> The  $\text{H}_2$  release reaction from the coiled structure is exothermic by 10–12 kcal/mol for  $n = 3$ , consistent with previous calculations.<sup>62</sup>

**IV. Intermolecular Dehydrogenation of  $\text{NH}_3\text{BH}_3$  Molecules.** All the transition state calculations so far focus on *intramolecular* dehydrogenation from the monomer and from the oligomers. As shown by the CPMD simulation and the transition state searches, the  $\text{NH}_3\text{BH}_3$  molecule can undergo an intramolecular hydrogen-transfer to form  $\text{NH}_2\text{BH}_2$  with  $\text{H}_2$  released. Then the  $\text{NH}_2\text{BH}_2$  molecules can easily dimerize to form the cyclic  $c\text{-(NH}_2\text{BH}_2)_2$  molecule through opening of the  $\text{B}=\text{N}$  double bonds (see above). Besides intramolecular dehydrogenation, *intermolecular* dehydrogenation is another possible channel for  $\text{H}_2$  release. Here we are interested in determining: (a) if the cyclization of two  $\text{NH}_3\text{BH}_3$  molecules can be achieved through a one-step reaction, that is, forming a  $c\text{-(NH}_2\text{BH}_2)_2$  molecule with two simultaneous  $\text{H}_2$  releases; (b) if two  $\text{NH}_3\text{BH}_3$  molecules can pass through a head-to-tail transition state to form oligomers via intermolecular dehydrogenation. We have searched for the transition state of two  $\text{NH}_3\text{BH}_3$  molecules oriented in various relative positions, and the results are presented in this section.

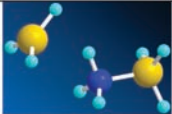
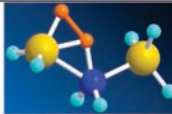
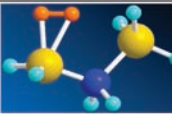
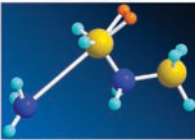

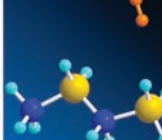
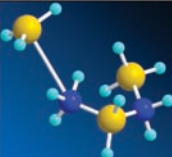
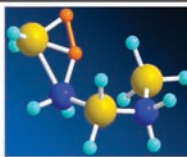
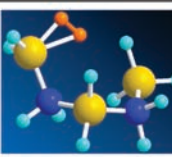
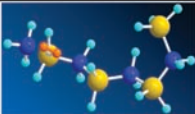
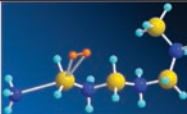
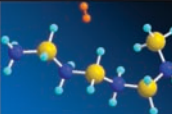
The transition state search of direct dehydrogenation of two  $\text{NH}_3\text{BH}_3$  molecules arranged in a face-to-face pattern (reactant side of Figure 2) indicates that an unusual *associative* transition state exists, in which two intermolecular hydrogen-transfer processes occur simultaneously. Figure 2 illustrates the potential energy curve of the dual hydrogen-transfer process, with the structures of the reactant, transition-state, and product being shown in the inset. The transition state has an imaginary mode at  $995i \text{ cm}^{-1}$ , significantly smaller than that of the hydrogen-transfer transition state of the  $\text{NH}_3\text{BH}_3$  molecule. This transition state features two DHIs with B atoms, where the optimized H–B distances of  $\text{R-BH}_2(\eta^2\text{-H}_2)$  are 1.44 Å and 1.70 Å and the B–N distance 1.50 Å, similar to those of **1-TS2**. The calculated ADF PW91 energy barrier of this transition state is 34.3 kcal/mol with respect to the  $\text{NH}_3\text{BH}_3$  dimer, and it is slightly increased to 38.2 kcal/mol based on a B3LYP calculations using Gaussian 98.

(63) Pan, L. L.; Li, J.; Wang, L.-S. *J. Chem. Phys.* **2008**, *129*, 024302.

(64) Matus, M. H.; Anderson, K. D.; Camaioni, D. M.; Autrey, S. T.; Dixon, D. A. *J. Phys. Chem. A* **2007**, *111*, 4411.



**Table 6.** Structures and Energies of the Reactants, Transition States, and Products for Formation of the Oligomers  $n = 2$  and  $n = 3$ <sup>a</sup>

oligomer	R	TS	$\Delta E_{TS}$	$\nu_{TS}$	P	$\Delta E_P$
n=2			12.4	865i		-14.9
			2.0	278i		-18.4
n=3			16.9	1086i		-12.9
			26.4	177i		+0.2

<sup>a</sup>All the energies (in kcal/mol) are calculated using ADF PW91/TZ2P and are relative to the energies of the reactants. Imaginary frequencies of the transition states are listed. The color code: B, yellow; N, blue; H, cyan; dihydrogen H, orange.

The IRC calculations show that the transition state indeed connects the  $\text{NH}_3\text{BH}_3$  dimer as a reactant and the  $2(\text{NH}_2\text{BH}_2 + \text{H}_2)$  molecules as products. The  $\text{NH}_2\text{BH}_2$  molecules can easily form the  $c\text{-(NH}_2\text{BH}_2)_2$  molecule via the transition state **2-TS2**. Whereas the dual hydrogen transfer, which leads to the simultaneous release of two  $\text{H}_2$  molecules, is very interesting, the formation of  $c\text{-(NH}_2\text{BH}_2)_2$  via one-step direct dimerization of two head-to-tail arranged  $\text{NH}_3\text{BH}_3$  molecules was not found experimentally, consistent with the relatively high activation barrier. Instead two steps are needed to accomplish the cyclization from two  $\text{NH}_3\text{BH}_3$  molecules. The overall reaction  $(\text{NH}_3\text{BH}_3)_2 \rightarrow 2[\text{NH}_2\text{BH}_2 + \text{H}_2] \rightarrow c\text{-(NH}_2\text{BH}_2)_2 + 2\text{H}_2$  is highly exothermic because of the large H–H bond energy and the dimerization energy of  $c\text{-(NH}_2\text{BH}_2)_2$  (Table 3). The formation of DHI is the rate-determining step and it apparently requires too high an activation energy to occur at low-temperature thermal reactions.

Starting from different orientations of two  $\text{NH}_3\text{BH}_3$  molecules, we also searched for transition states of a single dehydrocoupling step to form the  $n = 2$  oligomer  $\text{NH}_3\text{BH}_2\text{—NH}_2\text{BH}_3$  and  $\text{H}_2$ , but all these calculations were unsuccessful. Many of these calculations converged to structures in which the **1-TS2** type transition state is bound to another  $\text{NH}_3\text{BH}_3$  molecule via a dihydrogen bond. The following IRC calculations confirm that such a transition state is in fact the same as the intramolecular hydrogen-transfer, and the effects of the second  $\text{NH}_3\text{BH}_3$  molecule on the barrier height and exothermicity are negligible ( $\sim 1$  kcal/mol). Therefore, other possible pathways have to be searched to unravel how the  $\text{H}(\text{NH}_2\text{BH}_2)_n\text{H}$  oligomers are formed.

**V. Formation Mechanisms of the Oligomers from  $\text{NH}_3\text{—BH}_3$ .** We have shown that the formation of oligomers via direct intermolecular dehydrogenation is difficult in thermal reactions. On the other hand, recent calculations

have shown that the B–N bond cleavage that yields  $\text{BH}_3$  and  $\text{NH}_3$  intermediates is a much faster reaction than intramolecular hydrogen-transfer.<sup>33,49</sup> We therefore investigated the  $\text{NH}_3\text{BH}_3$  molecule reacting sequentially with the  $\text{BH}_3$  and  $\text{NH}_3$  intermediates to form oligomers. The structures and energies of the reactants, transition states, and products for forming the  $\text{H}(\text{NH}_2\text{BH}_2)_n\text{H}$  oligomers  $n = 2$  and  $n = 3$  are listed in Table 6. There are four possible channels when  $\text{BH}_3$  and  $\text{NH}_3$  attack the  $\text{NH}_3\text{BH}_3$  molecule from either of its ends. It turns out that the reaction of  $\text{BH}_3$  on the N-site of  $\text{NH}_3\text{BH}_3$  molecule has the lowest barrier. As the  $\text{BH}_3$  moiety approaches the N-site, a hydrogen transfer occurs from N to B, forming a DHI-stabilized transition state with a partially formed B–N bond. The IRC calculation shows that through this transition state the  $\text{NH}_3\text{BH}_3 + \text{BH}_3$  reactants are transformed into a  $\text{BH}_3\text{NH}_2\text{—BH}_2(\eta^2\text{-H}_2)$  intermediate, which is energetically more stable than the reactants by 14.9 kcal/mol at the PW91 level of theory. The activation barrier of this reaction is only 12.4 kcal/mol, which is much lower than any of the hydrogen-transfer pathways discussed so far and even lower than the barrier for the B–N bond cleavage. In the next step, a  $\text{NH}_3$  molecule attacks the R- $\text{BH}_2(\eta^2\text{-H}_2)$  site, the  $n = 2$  oligomer is formed with one  $\text{H}_2$  molecule released. This second step is strongly exothermic ( $-18.4$  kcal/mol), and the activation barrier is only  $\sim 2$  kcal/mol, indicating that the second step will occur as soon as the dihydrogen intermediate is formed and  $\text{NH}_3$  becomes available. This might explain why little ammonia is released during the thermal decomposition despite B–N cleavage, because  $\text{BH}_3$  species readily attacks  $\text{NH}_3\text{BH}_3$  molecules to form the DHI intermediates, which can be instantly converted to the  $n = 2$  oligomers by  $\text{S}_\text{N}2$ -type substitution reaction through attack by  $\text{NH}_3$  molecules and release of  $\text{H}_2$  molecules. The dissociation energy of  $\text{NH}_3\text{BH}_3$  (staggered)  $\rightarrow \text{NH}_3 + \text{BH}_3$  is 31.7 kcal/mol

and the process  $2 \text{NH}_3\text{BH}_3 \rightarrow \text{H}(\text{NH}_2\text{BH}_2)_2\text{H} + \text{H}_2$  will be exothermic by 1.6 kcal/mol based on the reaction energies listed in Table 6. Therefore formation of the  $n = 2$  oligomer are thermodynamically favorable, with the dissociation of  $\text{NH}_3\text{BH}_3$  as the rate-determining step.

The  $n = 3$  oligomer can be formed through an analogous mechanism. As shown in Table 6, when the  $\text{BH}_3$  fragment attacks the  $\text{NH}_3$  head of the  $n = 2$  oligomers, the activation barrier of 16.9 kcal/mol is slightly larger than that of the first-step for  $n = 2$ . This transition state also features DHI, and the complete hydrogen transfer from N to B leads to the formation of a dihydrogen intermediate  $\text{H}(\text{BH}_2\text{NH}_2)_2\text{BH}_2(\eta^2\text{-H}_2)$ , with an energy release of  $-12.9$  kcal/mol. After the  $\text{NH}_3$  attack on the  $\text{R-BH}_2(\eta^2\text{-H}_2)$  site the  $n = 3$  oligomer is formed with the release of one  $\text{H}_2$  molecule. The energetic and barrier differences of the  $\text{NH}_3$  attacking to the intermediates for the  $n = 3$  and  $n = 2$  are somewhat unexpected. Because the dihydrogen molecule is only weakly bound to B, the imaginary frequency for the second transition state is quite small. One can imagine that all the  $n > 3$  oligomers can be formed through the same mechanism, here characterized only for  $n = 2$  and  $n = 3$ . Therefore we have found a two-step pathway for the formation of the  $\text{H}(\text{NH}_2\text{BH}_2)_{n+1}\text{H}$  oligomers through (i) the reactions of  $\text{BH}_3$  with  $\text{H}(\text{NH}_2\text{BH}_2)_n\text{H}$  to form an intermediate  $\text{H}(\text{BH}_2\text{NH}_2)_n\text{BH}_2(\eta^2\text{-H}_2)$  and (ii) the subsequent reaction of  $\text{H}(\text{BH}_2\text{NH}_2)_n\text{BH}_2(\eta^2\text{-H}_2)$  with  $\text{NH}_3$  to form  $\text{H}(\text{NH}_2\text{BH}_2)_{n+1}\text{H}$  and  $\text{H}_2$ .

**VI. Mechanistic Implications toward Hydrogen Release from PAB to form PIB.** There has been progress recently toward understanding the mechanisms for decomposition of solid  $\text{NH}_3\text{BH}_3$  (ammonia borane = AB) to form PAB,  $\text{H}(\text{BH}_2\text{NH}_2)_n\text{H}$ , and  $\text{H}_2$ .<sup>13,26</sup> On the other hand, much less is known of the mechanism for thermal hydrogen release in the “second step”, that is, PAB to form PIB  $\text{H}(\text{BHNH})_n\text{H} + \text{H}_2$ . These reactions occur at higher temperatures than the “first step”, as also shown from the CPMD simulations. It is often assumed, based only upon structural changes between PAB and PIB, that the decomposition reaction proceeds by intramolecular release of hydrogen through 1,2-elimination and cyclization pathways.<sup>65,66</sup> Here we will summarize some of the more probable mechanisms of hydrogen release from PAB to form PIB inferred from the calculations described here and the recent literature. Using the reaction energetics from Table 4 and those from Nutt and McKee<sup>18</sup> in their Figure 5 (p. 7641), we note that the dehydrocoupling reaction via hydrogen-transfer for the  $n = 3$  oligomer has a barrier (49.4 kcal/mol) that is too high to be competitive for hydrogen release given the lower-energy reaction pathways found by Nutt and McKee so long as there is a lower energy pathway to get from  $\text{NH}_3\text{BH}_2(\text{NH}_2\text{BH}_2)_x\text{NH}_2\text{BH}_3$  to the unsaturated species E2, ( $x = 1$ ),  $\text{NH}_2=\text{BH}(\text{NH}_2\text{BH}_2)_x\text{NH}_2\text{BH}_3$ . If we assume that the barrier to remove  $\text{H}_2$  from the “head” end of the  $n = 3$  oligomer, via taking one H atom from the  $\text{NH}_3$  and one H atom from the adjacent  $\text{BH}_2$ , is similar to the  $\sim 40$  kcal/mol barrier found for the  $n = 2$  oligomer, the resulting product state is the “E2” conformer found by Nutt and McKee. Another lower barrier is to form  $\text{NH}_3\text{BH}_2\text{-}$

$(\text{NH}_2\text{BH}_2)_x\text{NH}=\text{BH}_2$ , which is about 3 kcal/mol different in the barrier and has more favorable thermodynamics (see Table 4). This “E2” conformer then proceeds toward cyclotriborazane (CTB) with lower barriers ( $\sim 28$  kcal/mol) than the 49.4 kcal/mol barrier for cyclization of  $\text{NH}_3\text{BH}_2(\text{NH}_2\text{BH}_2)_x\text{NH}_2\text{BH}_3$ . It is interesting to note that the most difficult dehydrocoupling reaction is the removal of  $\text{H}_2$  from the middle of the oligomer (the barrier is  $\sim 60$  kcal/mol for  $n = 2$ ). Contrary to chemical intuition, these results suggest that 1,2-elimination of  $\text{H}_2$  from the middle of a PAB structure will not be an important reaction pathway leading to PIB, rather hydrogen release will be initiated from the terminal positions in the PAB oligomer chain ( $\sim 40$  kcal/mol) or through B–N scission pathways ( $\sim 28$  kcal/mol) in larger oligomers, leading to the formation of more active terminal links in the PAB structure, for example,  $\text{NH}_3\text{BH}_2\text{-}(\text{NH}_2\text{BH}_2)_x\text{NH}_2\text{BH}_3 \rightarrow \text{NH}_3(\text{BH}_2\text{NH}_2)_x\text{BH}_3 + \text{NH}_2\text{BH}_2$ . Zimmerman et al. reported that the  $n = 2$  oligomer can undergo B–N bond scission with  $\text{H}_2$  release to form a pair of aminoborane species ( $\sim 29$  kcal/mol).<sup>20</sup> These scission reaction pathways are consistent with aminoborane observed as a major species in the thermal decomposition of PAB.<sup>65</sup>

## Conclusions

We have performed systematic theoretical studies on the potential reaction pathways for thermal decomposition and dehydrogenation of a series of  $\text{H}(\text{NH}_2\text{BH}_2)_n\text{H}$  oligomers resulting from ammonia borane. The CPMD simulations at different temperatures provide essential information about possible intermediates and products of decomposition and dehydrogenation of ammonia borane. The subsequent DFT electronic structure calculations show that there are two types of transition states involving the B–N bond cleavage and/or hydrogen-transfer from an N-site to a B-site. The dihydrogen bonding, in which protic ( $\text{H}_\text{N}$ ) hydrogens interact with hydridic ( $\text{H}_\text{B}$ ) hydrogens, plays a vital role in stabilizing different structures of the reactants, transition states, and products, forming the dihydrogen interaction (DHI) within the  $\text{R-BH}_2(\eta^2\text{-H}_2)$  moiety accounting both for the formation mechanisms of the oligomers and for the dehydrogenation of ammonia borane.

The results of our theoretical investigations indicate that the  $\text{H}(\text{NH}_2\text{BH}_2)_{n+1}\text{H}$  oligomers are likely formed through reactions of the  $\text{H}(\text{NH}_2\text{BH}_2)_n\text{H}$  oligomers first with  $\text{BH}_3$  followed by reactions with  $\text{NH}_3$  and the release of  $\text{H}_2$ . The reactive  $\text{BH}_3$  and  $\text{NH}_3$  intermediates are formed through dissociation of  $\text{NH}_3\text{BH}_3$  with a barrier of about 30 kcal/mol. We also find that the dehydrogenation of the  $\text{NH}_3\text{BH}_3$  dimer encounters a barrier of about 35 kcal/mol, with the products being  $2(\text{NH}_2\text{BH}_2 + \text{H}_2)$ . The two  $\text{NH}_2\text{BH}_2$  molecules can form the  $c\text{-}(\text{NH}_2\text{BH}_2)_2$  molecule with a transition state of about 9 kcal/mol. The overall  $(\text{NH}_3\text{BH}_3)_2 \rightarrow c\text{-}(\text{NH}_2\text{BH}_2)_2 + 2\text{H}_2$  reaction is highly exothermic.

The dehydrogenation of the  $\text{H}(\text{NH}_2\text{BH}_2)_n\text{H}$  oligomers encounters significant barriers. The barriers for reactions involving the head and the tail sites are 25.2 and 40.9 kcal/mol for  $n = 2$  and 3, respectively, and the products have at least one B–N bond cleavage. The barriers for hydrogen transfer from N to the neighboring B atom across the chain of the oligomers are even higher, in the 37–59 kcal/mol range. For

(65) Geanangel, R. A.; Rabalais, J. W. *Inorg. Chim. Acta* **1985**, *97*, 59.

(66) Baumann, J.; Baitalow, F.; Wolf, G. *Thermochim. Acta* **2005**, *430*, 9.

$n = 3$ , a barrier for the dehydrocoupling reaction involving the terminal B and N sites is also significant (49.4 kcal/mol), but it leads to a remarkably stable product of cyclotriborazine,  $c\text{-(NH}_2\text{BH}_2)_3$ . This work provides further direction toward an improved understanding of the mechanism of hydrogen release from solid PAB. Further experimental and theoretical work is in progress toward addressing the outstanding issues.

**Acknowledgment.** We are grateful to Drs. John Linehan and Don Camaioni for helpful discussions. S.K. and G.S. acknowledge support from the U.S. Department of Energy, Office of Basic Energy Sciences, Chemical Sciences Division. J.L. and T.A. acknowledge support from DOE EERE Chemical Hydrogen Storage Center of Excellence. J.L. is also supported by NKBRSF

(2006CB932300, 2007CB815203) and M.G. was supported by a Marie Curie project MIRG-CT-2007-046477 within the 6th European Community Framework Programme. This research was performed in part using the Molecular Science Computing Facility in the William R. Wiley Environmental Molecular Sciences Laboratory, a national scientific user facility sponsored by the U.S. Department of Energy's Office of Biological and Environmental Research and located at the Pacific Northwest National Laboratory. Pacific Northwest National Laboratory is operated for the Department of Energy by Battelle.

**Supporting Information Available:** Optimized geometries of the CPMD final structures of the  $(\text{NH}_3\text{BH}_3)_n$  clusters ( $n = 1, 4$ ) and the  $\text{H}(\text{NH}_2\text{BH}_2)_{n+1}\text{H}$  oligomers. This material is available free of charge via the Internet at <http://pubs.acs.org>.